lubricants

MDPI

Article

Evaluation of a Commercial MoS_2 Dry Film Lubricant for Space Applications

Duval A. Johnson [1,*], Marcello Gori [1], Azhar Vellore [1], Andrew J. Clough [2], Scott D. Sitzman [2], Jeffrey R. Lince [3] and Ashlie Martini [4]

[1] NASA Jet Propulsion Laboratory, California Institute of Technology, 4800 Oak Grove Dr, Pasadena, CA 91109, USA
[2] The Aerospace Corporation, 2310 E. El Segundo Blvd., El Segundo, CA 90245, USA
[3] Space Tribology Consulting, Inc., Culver City, CA 90232, USA; jeff@spacetribology.com
[4] Department of Mechanical Engineering, University of California Merced, 5200 N. Lake Road, Merced, CA 95343, USA; amartini@ucmerced.edu
* Correspondence: duval.a.johnson@jpl.nasa.gov

Abstract: Molybdenum disulfide coatings, particularly Microseal 200-1, have been extensively used as dry film lubricants for actuating mechanisms in space applications. Although Microseal 200-1 has historically been a popular choice for space missions, recent assessments indicate a need for reexamination. This study evaluates sliding friction in air and dry gaseous nitrogen atmospheres at ambient temperatures with both linear reciprocating and rotary unidirectional tribo-tests. Measurements are performed for Microseal 200-1 applied on substrates and surface treatments commonly used in aerospace components, particularly stainless steel and a titanium alloy. Our findings indicate that the friction of stainless steel balls sliding on Microseal 200-1-coated disks is significantly influenced by the environment as well as the disk substrate material. The average friction coefficient ranges from 0.12 to 0.48 in air and from 0.04 to 0.41 in dry gaseous nitrogen, and the amount of friction is consistently much higher for the Microseal 200-1 on the stainless steel than on the titanium alloy. Microscopy and surface analyses, including scanning electron microscopy, energy-dispersive X-ray spectroscopy, and X-ray fluorescence, of the coatings on stainless steel substrates reveals that the coatings are sparse and relatively thin, likely a key factor contributing to their high friction. This insight underscores the substrate dependence of this widely used coating and highlights the importance of detailed tribological testing in accurately assessing the tribological performance of commercial dry film lubricants, a key step towards improving the reliability and effectiveness of actuating mechanisms for space applications.

Keywords: MoS_2; dry film lubricant; space tribology; Microseal 200-1; friction coefficient

Citation: Johnson, D.A.; Gori, M.; Vellore, A.; Clough, A.J.; Sitzman, S.D.; Lince, J.R.; Martini, A. Evaluation of a Commercial MoS_2 Dry Film Lubricant for Space Applications. *Lubricants* **2024**, *12*, 307. https://doi.org/10.3390/lubricants12090307

Received: 31 July 2024
Revised: 27 August 2024
Accepted: 28 August 2024
Published: 31 August 2024

1. Introduction

Actuating mechanisms that operate in extraterrestrial environments must withstand extreme conditions, including high G-force vibrations, significant temperature fluctuations, and low pressure and vacuum environments. These mechanisms also need to survive periods of time (which can include either intended or unavoidable relative motion) in ambient terrestrial environments. In such applications, traditional liquid and semi-solid lubricants are often impractical or ineffective. Instead, dry film lubricants (DFLs) have become the standard [1,2], with molybdenum disulfide (MoS_2) being the most prevalent choice for space applications due to its proven efficacy in satellites and spacecrafts [2–5]. Among the various MoS_2-based coatings available, Microseal 200-1 (MS 200-1), produced by E/M Coating Services, has gained prominence. This is an impinged coating made of finely powdered MoS_2 that contains a small amount of inorganic binder, corresponding to SAE AMS2526 [6].

Initially selected as "the safest compromise coating" for Mariner 69's hydrazine expulsion bladders [7], its use by NASA has expanded to various sliding and rolling surfaces for components including bearings, springs, and gears, due to its low coefficient of friction (COF), which has been reported to be typically between 0.02 and 0.06 depending on the load and the substrate material [8]. Microseal 200-1 has also been adopted by other space agencies, including the European Space Agency's Nanokhod Microrover, where it was applied on all contact surfaces and bearings [9,10]. Microseal 200-1 has also been used as a benchmark for assessing the friction performance of new coating materials [11,12]. Notably, Microseal 200-1 was recently used in NASA's Mars rover Perseverance, demonstrating continued trust in Microseal 200-1 for high-stakes extraterrestrial missions.

Despite its widespread application, Microseal 200-1 is a MoS_2-based coating and, as such, has the limitations inherent to this material. Particularly, interactions with air are known to adversely affect the tribological performance of MoS_2 DFLs [3]. Chemical reactions between MoS_2 and oxygen can lead to the formation of MoO_3 [13]. Humidity is also problematic since water molecules can physically adsorb on the MoS_2 surface [14]. Both chemical reactions with oxygen and the physical adsorption of water can disrupt the easy shear ability of MoS_2 DFLs which decreases their lubricity [3,15–19]. Specifically for Microseal 200-1, a recent series of tribo-tests conducted on various space-relevant coatings and surface treatments revealed inconsistencies in their performances [20]. In particular, these tests, detailed in Vellore et al., raised concerns about Microseal 200-1's sensitivity to the substrate surface material and its inability to consistently achieve low levels of friction. However, the measurements on Microseal 200-1 in the study by Vellore et al. were performed in only select operating and environmental conditions, and the results were not plotted or analyzed. As such, Microseal 200-1 continues to be a favored choice for space mechanism components.

Our study aims to further characterize the tribological performance of Microseal 200-1 under various conditions. We first analyzed existing data to confirm the influence of substrate material on friction behavior. Then, we conducted new tests on two space mechanism-relevant materials, 440C stainless steel and Ti-6Al-4V titanium alloy, comparing the coating's performance under different speed and loading conditions using both rotary unidirectional and linear reciprocating sliding motion. Although post-test surface characterization confirmed that the coating on the stainless steel substrate was not completely removed during testing, the results indicated poorer friction performance than on the titanium alloy. Utilizing microscopy and surface characterization, we analyzed differences in the as-deposited coating's morphology and composition between the two substrates, which provided valuable insights for interpreting the results.

2. Methods

Friction was measured between 440C stainless steel balls of ¼ inch nominal diameter and Microseal 200-1-coated disks. The disks were made of either 440C stainless steel or a Ti-6Al-4V alloy. The Ti-6Al-4V samples underwent anodization by one of two vendors, either Danco or Tiodize, which is known to enhance the DFL's performance by improving surface hardness, chemical stability, and substrate–coating adhesion [21,22]. The average surface roughness of the disks prior to coating application ranged from 4 to 8 μin with non-directional surface lay; this very smooth surface condition was chosen to minimize the effect of substrate roughness on the results.

Microseal 200-1 was applied by Curtiss-Wright EM Coating Services using a proprietary approach involving projection of micro-size particles at fast speeds onto a sample surface to create an impinged coating that is then cured at high temperature. The coated disks were stored in bags purged with GN_2 to minimize interactions with ambient environmental conditions and were then tested immediately after opening. The roughness of the samples after coating was measured using a profilometer (Mitutoyo AVNAT with a 12AAC731 stylus having a 2 μm tip radius) to be 40 μin ± 15 μin.

Friction measurements were conducted using a ball-on-disk tribometer (Rtec Instruments, San Jose, CA, USA, MFT-5000; accuracy and resolution of ±20 mN and 6 mN, respectively) under ambient atmosphere and dry gaseous nitrogen (GN_2) conditions, at ambient temperature. The ambient air tests mimicked the conditions in a space flight assembly facility and the GN_2 tests mimicked the low humidity conditions of space. The relative humidity in the ambient air tests was not controlled and was measured to be between 30 and 45%. In the GN_2 tests, the relative humidity was kept below 0.2% throughout the experiments. In both ambient and GN_2 conditions, the temperature was in the range of 23–26 °C.

Two types of sliding motions were used in the tests: rotary unidirectional and linear reciprocating, mimicking the motion patterns in the target application. For rotary unidirectional tests, various loading and sliding speed combinations were selected to mimic the conditions in some of the Perseverance Mars rover's mechanisms. These included sliding speeds of 950 and 9.8 mm/s with maximum Hertzian contact pressures of 285 and 570 MPa for 440C, and sliding speeds of 980 and 10 mm/s with maximum Hertzian contact pressures of 265 and 585 MPa for Ti-6Al-4V. The linear reciprocating tests were conducted at 0.33 mm/s, with pressures set at 570 and 520 MPa for 440C and Ti-6Al-4V, respectively. The test parameters and conditions for each substrate material are summarized in Table 1.

Table 1. Summary of test parameters used in the tests conducted on Microseal 200-1-coated 440C and Ti-6Al-4V substrates. Cases identified with * were measurements performed in the previous study by Vellore et al. but plotted and analyzed here.

Substrate	Motion	Pressure (MPa)	Speed (mm/s)	Atmosphere	# Tests
440C *	Rotary Unidirectional	300	1000	Air	2
Ti-6Al-4V *	Linear Reciprocating	510	0.5	Air	2
440C	Linear Reciprocating	570	0.33	Air	1
440C	Linear Reciprocating	570	0.33	GN_2	1
Ti-6Al-4V	Linear Reciprocating	520	0.33	Air	1
Ti-6Al-4V	Linear Reciprocating	520	0.33	GN_2	2
440C	Rotary Unidirectional	285	950	Air	3
440C	Rotary Unidirectional	285	950	GN_2	3
440C	Rotary Unidirectional	570	9.8	Air	1
440C	Rotary Unidirectional	570	9.8	GN_2	1
Ti-6Al-4V	Rotary Unidirectional	265	980	Air	3
Ti-6Al-4V	Rotary Unidirectional	265	980	GN_2	4
Ti-6Al-4V	Rotary Unidirectional	585	10	Air	2
Ti-6Al-4V	Rotary Unidirectional	585	10	GN_2	1

Throughout these tests, the coefficient of friction (COF) was continuously recorded. The unidirectional test data were processed using a moving mean with a stencil of 150 points, while the linear reciprocating data required correction for friction force bias due to misalignment between the force transducer and the sample surface [23], followed by averaging using a moving mean with a stencil of 250 points.

Post-test, the coating morphology and chemical composition of both substrates were examined using scanning electron microscopy (SEM) and energy-dispersive X-ray spectroscopy (EDS). Detailed SEM and EDS analyses were performed on focused ion beam (FIB)-cut samples. Additionally, X-ray fluorescence (XRF) analysis was conducted in the worn region of the coating of a 440C sample to gain further insights.

3. Results

Initially, we reevaluated the results of tests on Microseal 200-1 presented in a previous study by Vellore et al., who reported the data only, i.e., they have not yet been fully analyzed [20]. The processed data, shown in Figure 1, reveals distinct friction behaviors between the two different substrate materials. Notably, the COF in the rotary unidirec-

tional tests on Microseal 200-1 coated 440C was significantly higher than that in the linear reciprocating tests on Microseal 200-1 coated anodized Ti-6Al-4V. Also, while the COF was relatively stable during the Ti-6Al-4V tests, the friction started to increase after approximately 7.5 m of sliding in the 440C tests. Further, the relative motion and load/speed conditions differed between the tests on the two substrates, making a direct comparison of the substrates difficult.

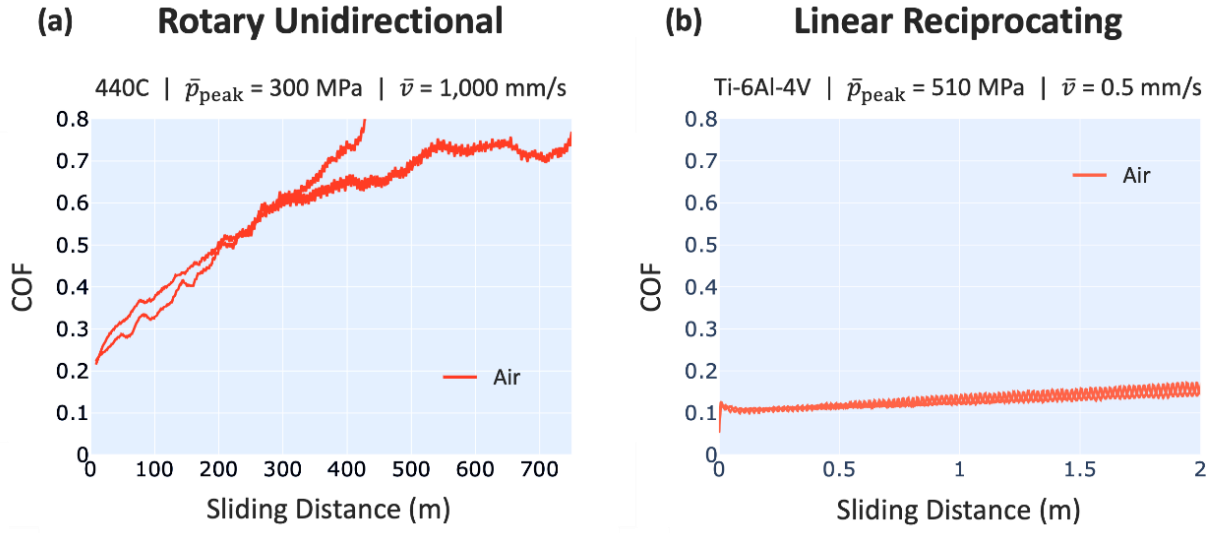

Figure 1. Coefficient of friction as a function of sliding distance in an ambient atmosphere: (**a**) rotary unidirectional tests on Microseal 200-1-coated 440C and (**b**) linear reciprocating tests on Microseal 200-1-coated anodized Ti-6Al-4V, as performed by Vellore et al. [20].

These findings prompted further comparative tests between 440C stainless steel and anodized Ti-6Al-4V. The results from these linear reciprocating tests are displayed in Figure 2. In Figure 3, repeated test data are combined into a single box plot, calculated from the data in Figure 2 excluding the initial 0.2 m of run-in. These figures show that environmental factors played a significant role, with a much lower COF observed in the GN_2 atmosphere compared to the ambient atmosphere, aligning with previous studies reporting the degradation of MoS_2's performance in humid air due to the adsorption of water [3,15,16]. Here, for 440C, the average friction coefficient was 39% lower in GN_2 than in air; it was 67% lower in GN_2 for Ti-6Al-4V. Comparing the two substrates, the friction coefficient on the titanium alloy was lower and more stable than that on the 440C steel, with the average COF in air for 440C being over 0.3, compared to 0.12 for Ti-6Al-4V. In GN_2, these values were 0.22 for 440C and 0.04 for Ti-6Al-4V.

To ensure that our findings were not specific to linear reciprocating motion, we also conducted rotary unidirectional sliding tests on the same Microseal 200-1-coated substrate materials. The results from these rotary unidirectional tests are displayed in Figure 4. Figure 5 consolidates the findings in a box plot format to facilitate comparison. Conducted at two different contact pressure and speed conditions, the data indicate a minor pressure/speed dependence within the tested range where the mean COF is slightly higher at lower pressures and faster speeds. There is also more variation in the data at the lower pressures and faster speeds, likely attributable to non-flatness of the disk samples (the top and bottom of the disks not perfectly parallel) which affects friction more under those conditions. Overall, the results mirrored the linear reciprocating data, showing a lower COF in GN_2 for both substrates and a more stable and lower COF for the titanium alloy compared to the 440C substrate.

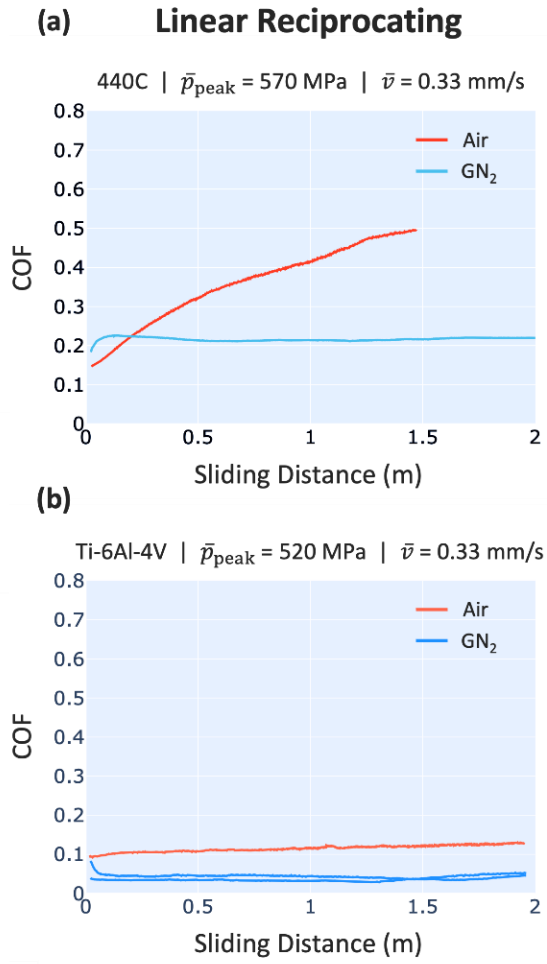

Figure 2. Friction coefficient versus sliding distance in air (red) and dry GN_2 (blue) atmospheres for linear reciprocating tests on (**a**) Microseal 200-1 coated 440C stainless steel and (**b**) Microseal 200-1 coated anodized Ti-6Al-4V alloy.

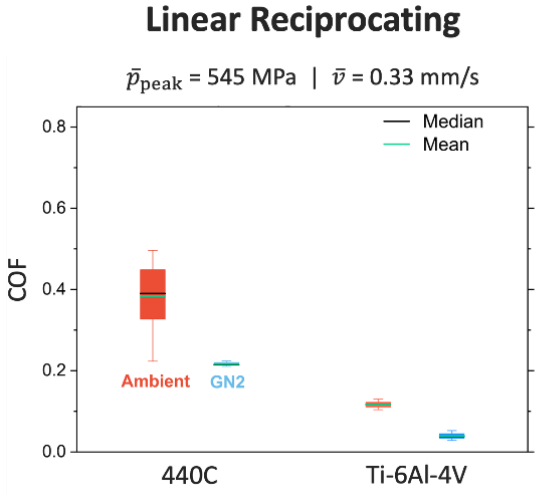

Figure 3. Summarized friction coefficients from linear reciprocating tests on Microseal 200-1-coated 440C stainless steel and anodized Ti-6Al-4V alloy in air (red) and GN_2 (blue). The box plots highlight the relative performance across substrates and environments.

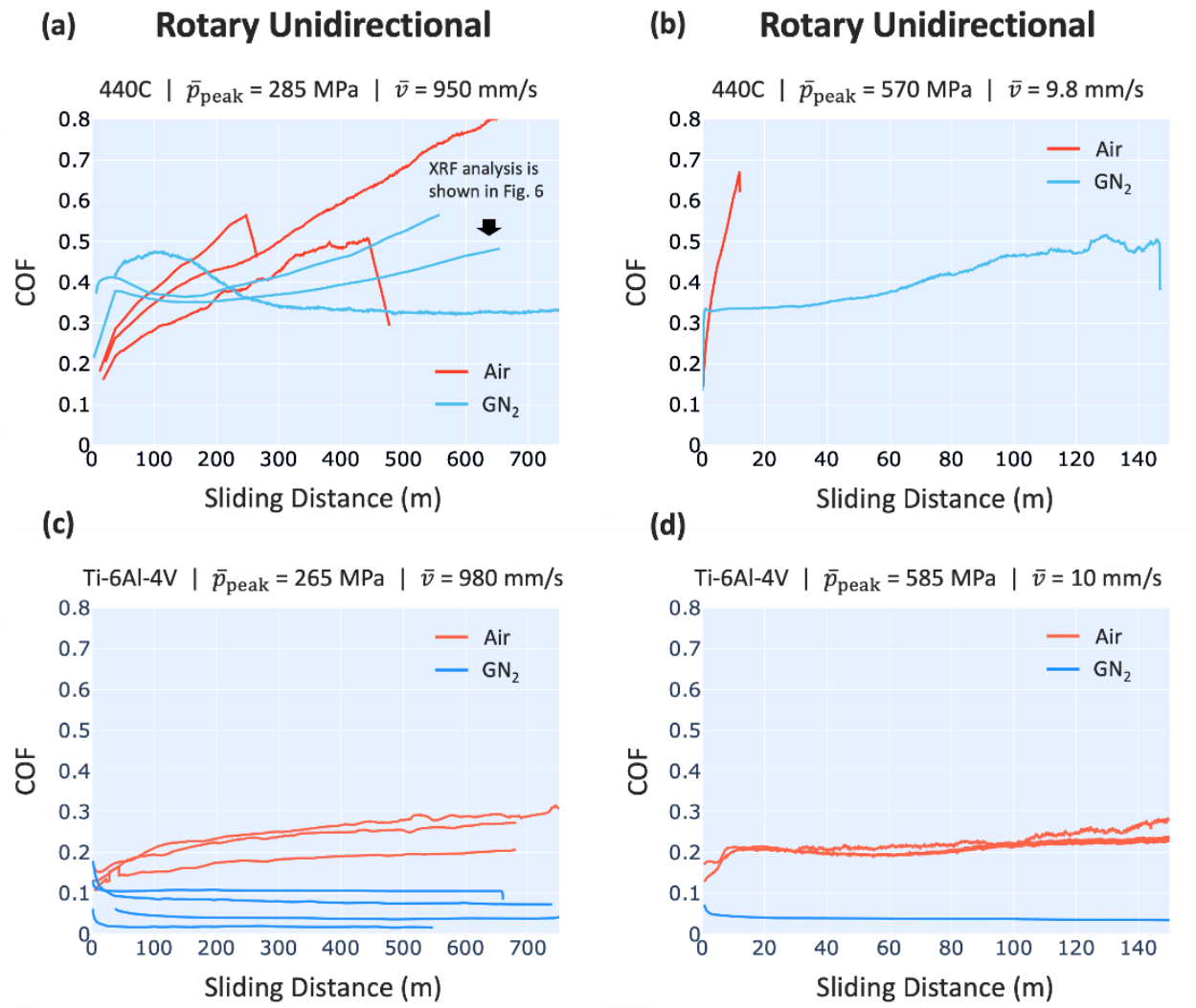

Figure 4. Friction coefficients from rotary unidirectional sliding tests on (**a**,**b**) Microseal 200-1-coated 440C stainless steel and (**c**,**d**) Microseal 200-1-coated anodized Ti-6Al-4V alloy in air (red) and GN_2 (blue). The left plots (**a**,**c**) correspond to tests run at lower peak contact pressures and higher speeds than the tests shown in the right plots (**b**,**d**).

The NASA Lubrication Handbook (1985) [8] reported Microseal 200-1 sliding friction coefficients of 0.02 to 0.06 in air and "limited or low" coefficients in a vacuum, and that the reported values vary "depending on load and substrate surface". This substrate dependence was evident in our study as well, with the average unidirectional COF (Table 1) in air being above 0.47 for 440C and 0.23 for Ti-6Al-4V; in GN_2, these values were 0.41 for 440C and 0.06 for Ti-6Al-4V. For reciprocating tests, the average COF in air was 0.38 for 440C and 0.12 for Ti-6Al-4V; in GN_2, these values were 0.22 for 440C and 0.04 for Ti-6Al-4V. The friction was consistently higher on the 440C than on the Ti-6Al-4V and the difference between the two substrates was more significant in GN_2 than in air.

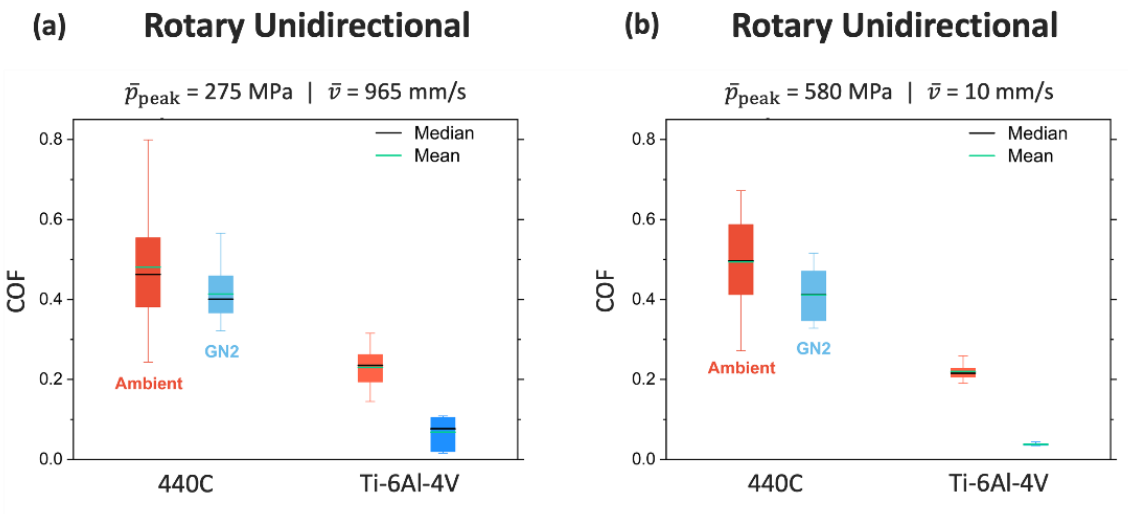

Figure 5. Comparative frictional analysis from unidirectional tests at (**a**) lower pressure and higher speed or (**b**) higher pressure and lower speed on Microseal 200-1-coated 440C stainless steel and Microseal 200-1-coated anodized Ti-6Al-4V alloy in air (red) and GN_2 (blue). The data are consistent with results from the linear reciprocating tests, confirming the difference in frictional performance between substrates and environmental conditions.

An XRF analysis was conducted on one of the wear tracks after a cumulative sliding distance of approximately 691 m to verify the coating's persistence throughout the test. This test was performed on a DFL-coated 440C coupon, which underwent unidirectional testing in a GN_2 atmosphere at a 285 MPa load and a 950 mm/s sliding speed. The upper left inset of Figure 6 is an optical microscope image of the wear track suggesting partial wear-off of the coating during testing. This observation aligns with the high friction coefficient exhibited by the corresponding friction trace in the upper left panel of Figure 4, implying DFL failure. XRF was performed in the area marked by a yellow star in the wear track image in the inset of Figure 6. The XRF data confirm the presence of MoS_2 in the wear track for the entirety of the test. Additionally, the XRF analysis indicates elevated levels of chromium and iron, which are attributable to wear of either the ball or the 440C substrate following DFL failure; the latter explanation is supported by the patchy appearance of the wear scar in the inset in Figure 6.

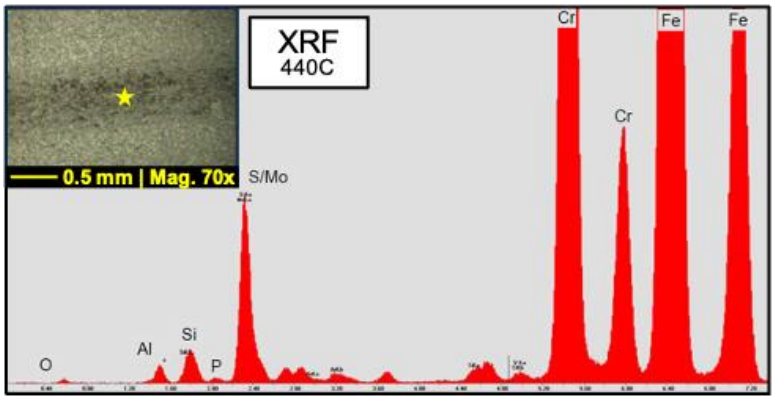

Figure 6. X-ray Fluorescence (XRF) analysis carried out on the wear track area marked by the yellow star in the upper left inset. The inset displays an optical microscope image of the region where the XRF measurement took place identified by a star. The analysis followed a ball-on-disk tribometer test on a Microseal 200-1 coated 440C substrate, conducted in GN_2 atmosphere with a peak contact pressure of 285 MPa and a sliding speed of 950 mm/s. The friction coefficient for this test is shown in the upper left panel of Figure 4.

Further microscopy on untested coatings was performed to understand the substrate-dependent performance of Microseal 200-1. SEM and EDS images of the untested coatings, presented in Figure 7, were acquired to characterize the morphology and chemical composition of the DFL-coated surfaces. The EDS map shown in Figure 7 reveals the presence of sulfur (from the MoS_2), along with aluminum and silicon. The presence of aluminum is attributed to residual alumina impurities from grit blasting performed on the substrate prior to DFL application. The presence of silicon may be due to the silicate in the inorganic binder used in the Microseal 200-1 deposition. In the case of the Ti-6Al-4V alloy, the notable presence of silicon in the bottom right panel of Figure 7 (in pink) may also be attributable to the anodizing process, which forms a layer composed of Ti oxides and Si oxides.

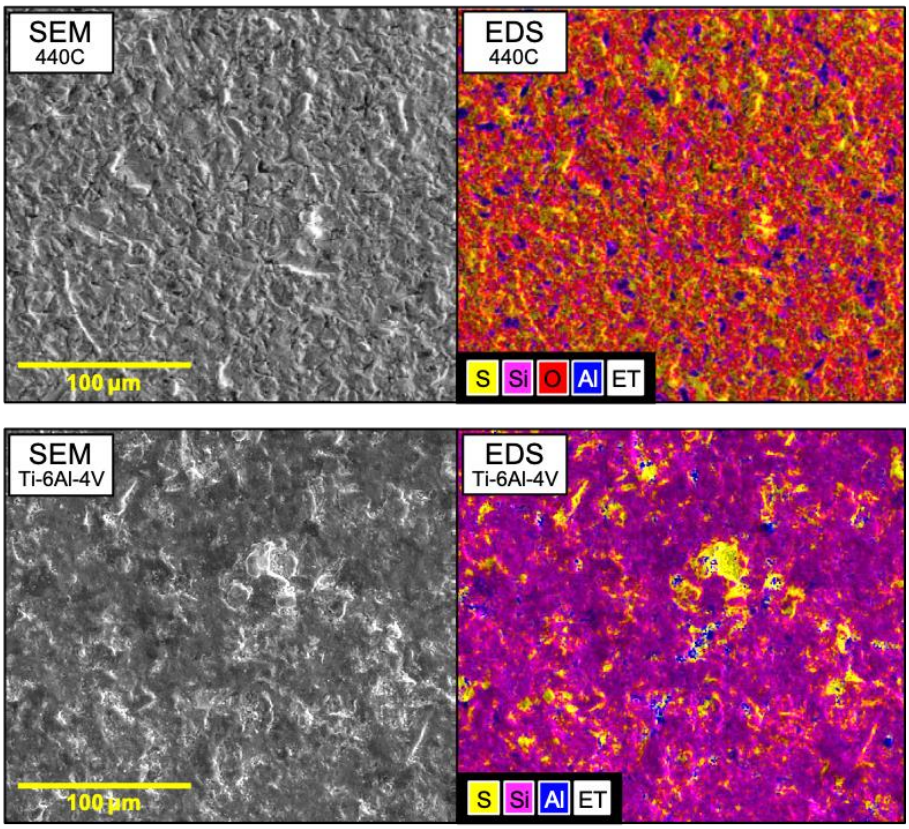

Figure 7. Surface morphology and chemical composition of Microseal 200-1 DFL coatings on 440C (**top panels**) and Ti-6Al-4V (**bottom panels**) substrates. SEM image (**left**) and EDS overlay (**right**) reveal the surface compositions before testing.

The SEM images in Figure 7 show rough surfaces for both 440C and Ti-6Al-4V substrates, with undulations on the order of tens of microns. FIB-cut cross-sections of the coatings provided additional information about the distribution of Microseal 200-1 coating thickness and composition on both substrates, with SEM and SEM/EDS overlays. The results are shown in Figures 8 and 9, for 440C and anodized Ti-6Al-4V substrates, respectively. Comparison of the SEM images in the left panels in Figures 8 and 9 indicates that 440C has a more irregular surface than Ti-6Al-4V. This surface roughness could partly explain Microseal 200-1's overall higher than expected friction and, particularly, its poorer performance on 440C compared to Ti-6Al-4V.

The SEM/EDS overlays in the right images of Figures 8 and 9 enable a comparison of the compositions of the coatings on the two different substrates. Notably, aluminum is present in both coatings, highlighted in red and pink in Figure 8 and green in Figure 9, with a significant amount of silicon detected in the coating on the Ti-6Al-4V substrate (shown in blue in Figure 9) attributed to the anodized layer and/or silicate binder. On both substrates,

Microseal 200-1 appears as pockets of sulfur, depicted in yellow in the SEM/EDS overlays of the FIB-cut sections.

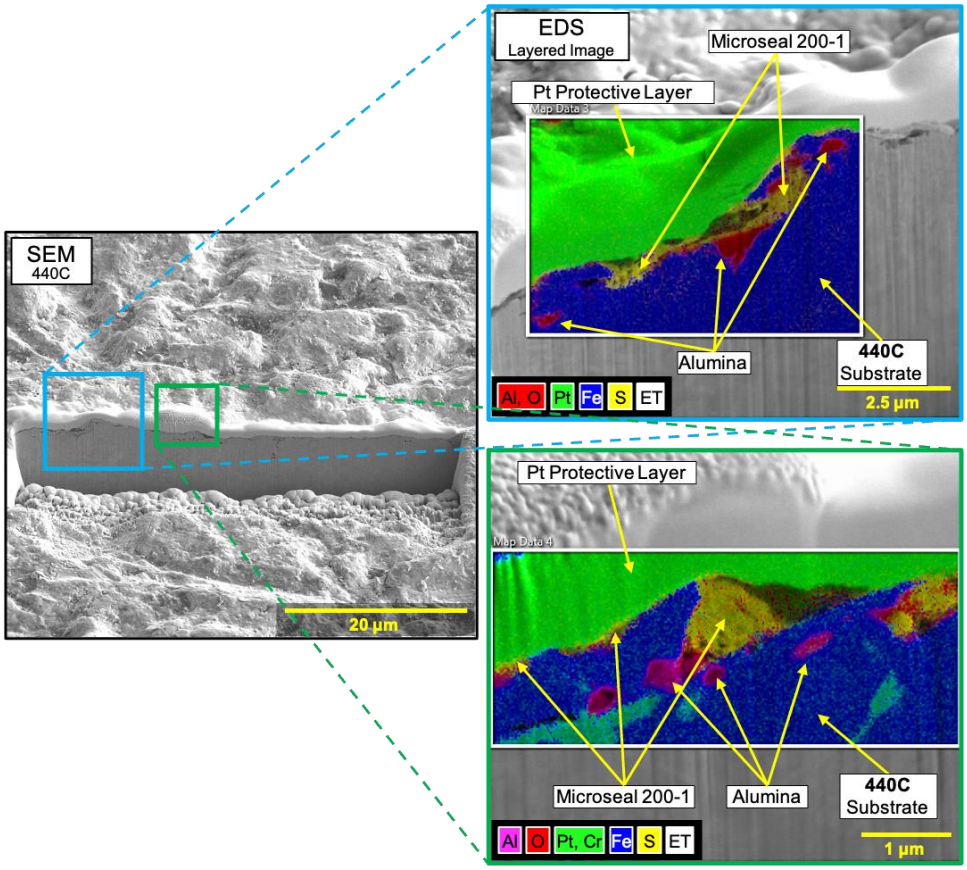

Figure 8. SEM and EDS images of FIB-cut cross-sections from the DFL-coated 440C stainless steel samples. The left figure is the SEM image, and the right figures are close-up SEM images with EDS overlays from two different locations on the FIB-cut section.

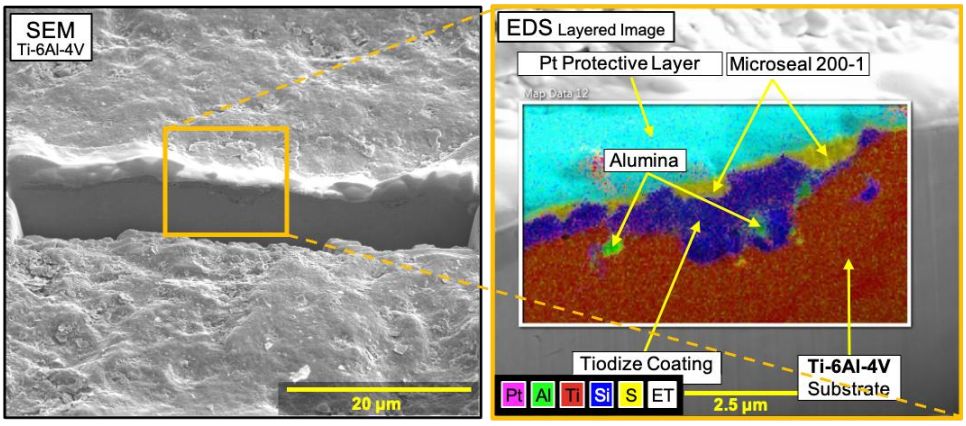

Figure 9. SEM and EDS images of FIB-cut cross-sections from the DFL-coated anodized Ti-6Al-4V alloy samples. The left figure is the SEM image, and the right figure is a close-up SEM image with an EDS overlay from one location on the FIB-cut section.

However, there are also differences between the two substrates. Notably, the coating material on the titanium alloy, including both the Microseal 200-1 and the anodizing layer, is approximately 2.5 µm thick. As seen in Figure 9, the coating is not uniform, and the majority is the anodizing layer. However, Figure 9 also suggests the presence of a continuous thin

layer of Microseal 200-1 on the topmost surface, in addition to the thicker patches. On the 440C substrate, the coating is even less uniform with no continuous layer of Microseal 200-1, as shown in Figure 8. Further, the coating on 440C is very thin, ranging from 0 to only about 1 μm. This thin and uneven application of Microseal 200-1 on the 440C may explain the poor DFL performance observed on this substrate.

These differences between the Microseal 200-1 on the 440C vs. the anodized Ti-6Al-4V substrates seen in the microscopy reflect the drastic difference in the tribological performance of the DFL on these two substrates. However, the origins of the differences cannot be inferred directly from our results. The fact that no binder species were detected on the 440C could point to poor adherence of the coating to that substrate. However, the same determination could not be made on the Ti-6Al-4V because the binder elements are also found in the anodize layer and so their presence in the coating could not be isolated.

4. Conclusions

Our evaluation of Microseal 200-1, an MoS_2 dry film lubricant, reveals critical insights into its tribological performance under conditions relevant to space applications. This study underscores the significant influence of substrate material and surface treatment on DFL effectiveness, with notable differences between 440C stainless steel and Ti-6Al-4V titanium alloy substrates.

The friction performance of Microseal 200-1 varied dramatically with the substrate material. The coatings on the titanium alloy substrates consistently demonstrated lower and more stable coefficients of friction compared to the coatings on the stainless steel substrates. Additionally, the significant difference in friction in tests run in ambient air compared to those run in GN_2 confirms the coating's vulnerability to humid air environments.

Microscopy and XRF characterization, coupled with FIB cross-sectional analysis, revealed uneven and thinner coating application on stainless steel substrates, along with irregular surface topography. These factors correlate with the suboptimal performance of the Microseal 200-1 on the 440C. In contrast, the thicker, more continuous Microseal 200-1 on the titanium alloy resulted in a better frictional behavior.

In summary, our study shows that, while Microseal 200-1 remains a viable DFL, its overall performance depends on operating and environmental conditions as well as substrate material. Understanding these dependencies is crucial for the selection and application of MoS_2-based DFLs. Finally, the results encourage future work aimed at comprehensively characterizing and then controlling the substrate dependence to produce DFLs that deliver reliable and durable performances in space applications.

Author Contributions: Conceptualization, D.A.J. and J.R.L.; methodology, A.J.C., J.R.L., and D.A.J.; formal analysis, A.V. and M.G.; investigation, A.J.C., S.D.S., and A.V.; writing—original draft preparation, A.M. and M.G.; writing—review and editing, A.J.C., S.D.S., J.R.L., M.G., and A.M.; visualization, A.J.C., S.D.S., and M.G.; project administration, D.A.J. All authors have read and agreed to the published version of the manuscript.

Funding: This research was partially conducted at the Jet Propulsion Laboratory, California Institute of Technology, under NASA sponsorship (80NM0018D0004). Reference herein to any specific commercial product, process, or service by trade name, trademark, manufacturer, or otherwise, does not constitute or imply its endorsement by the United States Government or the Jet Propulsion Laboratory, California Institute of Technology.

Data Availability Statement: The raw data supporting the conclusions of this article will be made available by the authors on request.

Acknowledgments: The authors would like to thank Stephen V. Didziulis for helpful advice and discussions about solid lubricant performance as well as Samuel Leventini for assistance with data compilation and manuscript references.

Conflicts of Interest: Authors Andrew J. Clough and Scott D. Sitzman were employed by The Aerospace Corporation. Author Jeffrey R. Lince was employed by Space Tribology Consulting, Inc. The remaining authors declare that the research was conducted in the absence of any commercial or financial relationships that could be construed as a potential conflict of interest.

References

1. Lince, J.R. Effective Application of Solid Lubricants in Spacecraft Mechanisms. *Lubricants* **2020**, *8*, 74. [CrossRef]
2. Colbert, R.S.; Sawyer, G.W. Thermal dependence of the wear of molybdenum disulphide coatings. *Wear* **2010**, *269*, 719–723. [CrossRef]
3. Vaziriserehk, M.R.; Martini, A.; Strubbe, D.A.; Baykara, M.Z. Solid Lubrication with MoS2: A Review. *Lubricants* **2019**, *7*, 57. [CrossRef]
4. Scharf, T.W.; Prasad, S.V. Solid lubricants: A review. *J. Mater. Sci.* **2013**, *48*, 511–531. [CrossRef]
5. Gradt, T.; Schneider, T. Tribological Performance of MoS2 Coatings in Various Environments. *Lubricants* **2016**, *4*, 32. [CrossRef]
6. SAE International. SAE International. SAE International Material Specification. In *COATING, THIN LUBRICATING FILM, MOLYBDENUM DISULFIDE Impingement Applied*; SAE International: Warrendale, PA, USA, 1972. [CrossRef]
7. Repar, J. Flight and Experimental Expulsion Bladders for Mariner 69 Final Report. 1969. Available online: https://ntrs.nasa.gov/citations/19700005527 (accessed on 4 November 2023).
8. Mcmurtrey, E.L. *Lubrication Handbook for the Space Industry*; NASA Tech Briefs: New York, NY, USA, 1985. Available online: https://ntrs.nasa.gov/citations/19860022258 (accessed on 4 Nov 2023).
9. Schiele, A.; Romstedt, J.; Lee, C.; Henkel, H.; Klinkner, S.; Bertrand, R.; Rieder, R.; Gellert, R.; Klingelhofer, G.; Bernhardt, B.; et al. Nanokhod Exploration Rover—A Rugged Rover Suited for Small, Low-Cost, Planetary Lander Mission. *IEEE Robot. Autom. Mag.* **2008**, *15*, 96–107. [CrossRef]
10. Schiele, A.; Romstedt, J.; Lee, C.; Henkel, H.; Klinkner, S.; Bertrand, R.; Rieder, R.; Gellert, R.; Klingelhöfer, G.; Bernhardt, B.; et al. The NANOKHOD Microrover—Development of an Engineering Model for Mercury Surface Exploration. In Proceedings of the 8th International Symposium on Artificial Intelligence, Robotics and Automation in Space (i-SAIRAS 2005), Munich, Germany, 5–8 Septmeber 2005.
11. Scharf, T.W.; Diercks, D.R.; Gorman, B.P.; Prasad, S.V.; Dugger, M.T. Atomic Layer Deposition of Tungsten Disulphide Solid Lubricant Nanocomposite Coatings on Rolling Element Bearings. *Tribol. Trans.* **2009**, *52*, 284–292. [CrossRef]
12. Scharf, T.W.; Gorman, B.P.; Prasad, S.V.; Dugger, M.T. Conformal Tungsten Disulphide Solid Lubricant Nanocomposite Coatings on Rolling Element Bearings. In Proceedings of the Society for the Advancement of Material and Process Engineering Fall Conference, Dallas, TX, USA, 6–9 November 2006.
13. Jiang, Y.; Liu, Z.; Zhou, H.; Sharma, A.; Deng, J.; Ke, C. Physical adsorption and oxidation of ultra-thin MoS2crystals: Insights into surface engineering for 2D electronics and beyond. *Nanotechnology* **2023**, *34*, 405701. [CrossRef] [PubMed]
14. Bobbitt, N.S.; Curry, J.F.; Babuska, T.F.; Chandross, M. Water adsorption on MoS2 under realistic atmosphere conditions and impacts on tribology. *RSC Adv.* **2024**, *14*, 4717–4729. [CrossRef] [PubMed]
15. Babuska, T.F.; Curry, J.F.; Dugger, M.T.; Lu, P.; Xin, Y.; Klueter, S.; Kozen, A.C.; Grejtak, T.; Krick, B.A. Role of Environment on the Shear-Induced Structural Evolution of MoS2 and Impact on Oxidation and Tribological Properties for Space Applications. *ACS Appl. Mater. Interfaces* **2022**, *14*, 13914–13924. [CrossRef]
16. Arif, T.; Yadav, S.; Colas, G.; Singh, C.V.; Filleter, T. Understanding the independent and interdependent role of water and oxidation on the tribology of ultrathin molybdenum disulfide (MoS 2). *Adv. Mater. Interfaces* **2019**, *6*, 1901246. [CrossRef]
17. Curry, J.F.; Wilson, M.A.; Luftman, H.S.; Strandwitz, N.C.; Argibay, N.; Chandross, M.; Sidebottom, M.A.; Krick, B.A. Impact of Microstructure on MoS2 Oxidation and Friction. *ACS Appl. Mater. Interfaces* **2017**, *9*, 28019–28026. [CrossRef] [PubMed]
18. Khare, H.S.; Burris, D.L. The Effects of Environmental Water and Oxygen on the Temperature-Dependent Friction of Sputtered Molybdenum Disulfide. *Tribol. Lett.* **2013**, *52*, 485–493. [CrossRef]
19. Curry, J.F.; Ohta, T.; DelRio, F.W.; Mantos, P.; Jones, M.R.; Babuska, T.F.; Bobbitt, N.S.; Argibay, N.; Krick, B.A.; Dugger, M.T.; et al. Structurally driven environmental degradation of friction in MoS2 films. *Tribol. Lett.* **2021**, *69*, 96. [CrossRef]
20. Vellore, A.; Romero Garcia, S.; Johnson, D.A.; Martini, A. Ambient and Nitrogen Environment Friction Data for Various Materials & Surface Treatments for Space Applications. *Tribol. Lett.* **2021**, *69*, 10.
21. Zhou, X.; Ouyang, C. Anodized porous titanium coated with Ni-CeO_2 deposits for enhancing surface toughness and wear resistance. *Appl. Surf. Sci.* **2017**, *405*, 476–488. [CrossRef]
22. Budinski, K.G. Tribological properties of titanium alloys. *Wear* **1991**, *151*, 203–217. [CrossRef]
23. Burris, D.L.; Sawyer, W.G. Addressing Practical Challenges of Low Friction Coefficient Measurements. *Tribol. Lett.* **2009**, *35*, 17–23. [CrossRef]